Design of an Economic System for Improving the Performance of Three Types of PV Panels Using Solar Reflectors

Ramy Ahmed
Benha University,
Benha, Egypt
ramy.ahmed@hu.edu.eg

Ghada Amer
Benha University,
Benha, Egypt
ghada.amer@bhit.bu.edu.eg

Abstract—**Increasing generated power of PV panels is a major issue. Solar reflectors could be one of the cheapest and easiest ways to increase that power. It's lower in cost than adding more solar PV panels. By modeling a Simulink-MATLAB test module, to be derived from the real input factors. The measured and (estimated by calculations) components of irradiance are important for PV system modeling, and a dataset of hourly dropped irradiance, and some other meteorological records were collected from February 2013 till the time of writing this paper. This paper presents the differences in the power ratio of the 3 types of PV modules before and after applying reflecting panels, the type of commercial reflector is (semi-diffuse, flexible reflector made of an aluminized PET laminate). The values of short circuit current Isc and open-circuit voltage Voc were measured under different conditions. Data can be used to validate the comparison between the theoretical and real calculations of the output power, also to find the best type of the 3 types of PV modules (1-Polycrystalline. 2- Thin film. 3-Mono crystalline) to be operated under the Egyptian environmental conditions. Low-cost reflecting materials could be a good solution. The effect is more electrons are generated and hence the output power of the solar module increases. This paper founds that the highest average power ratio of the whole 3 types is for Thin-film modules which is (1.421441667) which means the output power after installing the reflectors is increased by about 42% from the basic output.**

I. INTRODUCTION

As the electricity produced by the PV module is directly related to the intensity of light irradiance it is receiving, so to increase the efficiency of the PV, a solar reflecting technique may be the cheapest solution. This would considerably decrease the cost of generated electricity. One way to improve the performance of PV systems is to use cost-effective reflecting materials. Due to less cost and simplified assembly of reflecting panels. The theoretical efficiency of a PV cell is close to being 30% to 40%. [4]

Reflectors are reflecting irradiance over the solar panel through dispersed light radiation. This is so useful especially on both sides of beak irradiance time, as it considerably enhances the output of the PV module. In addition to that, it also tends to minimize the drawbacks of hot spot development because of the focused intensity of radiation on some sections of the panel as those happened in the case of using mirrors, which does not only enhance the performance but also increases the lifetime of PV modules. Reflectors must be

installed at a certain angle, to reduce shading losses and allow maintenance access. Typically, the row spacing is designed to reduce shading losses that occur in the early morning and late afternoon. This study investigates the potential increase in energy yield and cell temperatures and develops new methodologies to accurately model the output of these systems. Besides, the new model analytically investigated the determination of temperature increases, and identification of the angle of diffused irradiance effects.

With the increase of interest in enhancing the generated power from solar-PV plants, promising paper and research related to the usage of reflector surfaces attached to the PV panels are emerging. paper discussing performance comparison of mirror reflected solar panel with tracking and cooling [1]. Also using the cooling mechanism to reduce the overheating effect was discussed [2]. A modeling method for handling with reflectors attached to the photovoltaic system for enhancing the performance with Non-Tracking Planar Concentrators: Experimental Results and Bi-Directional Reflectance Function (BDRF) Based Modelling. [3-10], A practical result of applying the experiments of attached mirrors and reflectors solar energy by reflection light method was discussed. [11-13]. The solar atlas of Egypt. [14]. Photovoltaic Efficiency is a very important factor with all other Concentrated Solar Power Fundamentals was discussed. [15-17]. Investigation of soiling effect on different solar mirror materials under the Moroccan climate. [18-19]. Lightweight Carbon Fiber Mirrors for Solar Concentrator Applications. [20]. A Simple Approach in Estimating the Effectiveness of Adapting Mirror Concentrator and Tracking Mechanism for PV Arrays in the Tropics. -the main target is to increase the daily energy generation from PV generators despite the fluctuating sun irradiance-. [21]. A Numerical Simulation of a Stationary Solar Field Augmented by Plane Reflector: Optimum Design Parameters. [22]. The mathematical model for the power generation from an arbitrarily oriented photovoltaic panel. [23]. A mathematical model for the power generation from arbitrarily oriented photovoltaic panels [24]. Progress in thin-film CIGS photovoltaics–Research and development, manufacturing, and applications", Progress in Photovoltaics: Research and Applications [26]. Cd-Free Cu(In,

Ga)(Se, S)2 Thin-Film Solar Cell With Record Efficiency of 23.35% [27].

II. METHODOLOGY AND MODELING

A system of 3 types of PV panels was selected, it's an already running system, the selection of the system was based on a huge logged data which is already stored and can be used as a reference of the research.

The location of the project is in Heliopolis University campus on the top roof of the building of the Faculty of Engineering. with a location coordinates: 30°09'11.7"N 31°25'57.4"E. Fig. 1

Fig.1. General view of the location

A. Description of the applied system

The solar system is installed on the roof of the Heliopolis University in Cairo. Three inverters are connected to a Sunny Island System with batteries.

Installation of 4.5 kWp demo plant with different types of modules and integration of local materials for mounting structure.
1) *Panels*
   The system consists of 3 sets of panels, each is consisting of one type of the PV, and generate an approximate power= of 1.5KW

   i. *Mono-Crystalline Panels*

   Consisting of 8 panels, Manufacturer: SOLAR WORLD, Country: Germany, $P_{max} = 175$ W, $V_{OC} = 44.4$ V, $V_{mpp} = 35.8$ V, $I_{SC} = 5.3$ A, $I_{mpp} = 4.9$ A, Total Power for the panels: 1400 W.

   ii. *Polycrystalline Panels*

   Consisting of 7 panels, Manufacturer: Canadian Solar, Country: Canada, $P_{max} = 235$ W, $V_{OC} = 36.9$ V, $V_{mpp} = 29.8$ V, $I_{SC} = 8.46$ A, $I_{mpp} = 7.9$ A, Total Power for the panels: 1645 W

   iii. *Thin Film Panels*

   Consisting of 21 panels, Manufacturer: First Solar Country: Germany, $P_{max} = 70$ W, $V_{OC} = 88$ V, $V_{mpp} = 65.5$ V, $I_{SC} = 1.23$ A, $I_{mpp} = 1.07$ A, Total Power for the panels: 1470 W

Total Power of the system=1400 (Mono Crystalline) +1645 (Polycrystalline)+1470 (Thin film) = 4515 W.

A reflectance model based on a BDRF (Bidirectional Reflectance Function) for the isotropic roughened surface is developed to predict the performance of the reflector system. (Fig. 2 a, b).
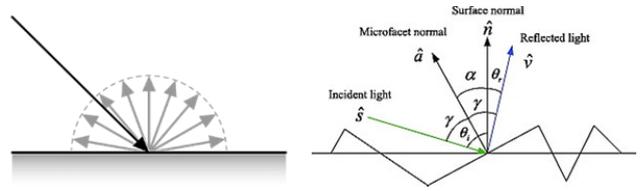

Fig.2 a   Fig.2 b

The model methodology presented in this paper uses the concepts of the BDRF (Bidirectional Reflectance Function) of non-ideal surfaces rather than traditional geometric optics. This methodology allows for the evaluation of non-specular reflectors in planar concentration systems, which has been shown to increase the energy yields from these systems. [1-5]

B. Effect of Temperature

While an increase in reflected irradiance is anticipated, which will increase generated electricity, it will also raise the temperature of the PV modules. The effect of higher temperatures on PV modules is that they harm the module's open-circuit voltage (V_{OC}), which will be considered in this article. [8]

PV panels, like all semiconductor products, are temperature sensitive. Temperature changes minimize a semiconductor bandgap, impacting most of the semiconductor material parameters. [9-12] A reduction in a semiconductor's bandgap as temperature rises can be interpreted as an increase in the energy of the material's electrons. As a consequence, less energy is required to break the bond. Reduced bond energy decreases the bandgap in the bond model of a semiconductor bandgap. As a consequence, raising the temperature decreases the band difference. [13-15].

1) Temperature dependence of the energy bandgap

As the temperature increases, the energy bandgap of semiconductors starts to narrow. When the magnitude of the atomic motions increases, the interatomic spacing increases, which helps to explain this phenomenon. as a result of the increased thermal energy [16], The linear expansion coefficient of a material is used to quantify this effect. The potential is seen by electrons in the material decreases as interatomic spacing increases, decreasing the size of the energy bandgap. [17–20] The bandgap is increased (decreased) when the interatomic distance is directly modulated, such as by applying high compressive (tensile) stress [24- 26].

The energy bandgap's temperature dependence has been calculated experimentally, yielding the following expression for E_g as a function of temperature T:

$$E_g(T) = E_g(0) - \frac{\alpha T^2}{T+\beta} \tag{1}$$

where $E_g(0)$, □ and □ are the fitting parameters. These fitting parameters are listed for germanium, silicon, and gallium arsenide in table (I) below: [21]

TABLE I. FITTING PARAMETERS FOR SEMICONDUCTORS

	Germanium	Silicon	GaAs
$E_g(0)$ [eV]	0.7437	1.166	1.519
□ [eV/K]	4.77 x 10^{-4}	4.73 x 10^{-4}	5.41 x 10^{-4}
□ [K]	235	636	204

The open-circuit voltage is the parameter in PV modules that are most impacted by temperature. [22.]

The effect of rising temperatures is represented in Fig. 3.

Fig.3. The effect of temperature on the IV characteristics of a solar cell

Since I_0 is temperature dependent, the open-circuit voltage decreases with temperature. From one side of a p-n junction, the equation for I_0 is:

$$I_0 = qA\frac{Dn_i^2}{LN_D} \quad (2)$$

where:
q is the electronic charge given on the constants page;
A is the area;
D is the diffusivity of the minority carrier given for silicon as a function of doping in the Silicon Material Parameters page;
L is the minority carrier diffusion length;
N_D is the doping; and
n_i is the intrinsic carrier concentration given for silicon in the Silicon Material Parameters page.

Many of the parameters in the above equation are thermodynamically favorable, but the intrinsic carrier concentration, n_i, has the most massive impact. The intrinsic carrier concentration is determined by the bandgap energy (lower bandgap energy corresponds to a significantly higher carrier concentration) and the energy that the carriers possess (with higher temperatures giving higher intrinsic carrier concentrations). The intrinsic carrier concentration can be calculated as follows: [27].

$$n_i^2 = 4\left(\frac{2\pi kT}{h^2}\right)^3 (m_e^* m_h^*)^{3/2} exp\left(-\frac{E_{Go}}{kT}\right) = BT^3 exp\left(-\frac{E_{Go}}{kT}\right) \quad (3)$$

where:
T is the temperature;
h and k are constants given in the constants page;
m_e^* and m_h^* are the effective masses of electrons and holes respectively;
E_{GO} is the band gap linearly extrapolated to absolute zero; and

B is a constant which is essentially independent of temperature.

Substituting these equations back into the expression for I_0, and assuming that the temperature dependencies of the other parameters can be neglected, gives:

$$I_0 = qA\frac{D}{LN_D}BT^3 exp\left(-\frac{E_{Go}}{kT}\right) \approx B'T^\gamma exp\left(-\frac{E_{Go}}{kT}\right) \quad (4)$$

Where B' is a constant that is independent of temperature. To account for the potential temperature dependencies of the other material parameters, a constant, γ, is used instead of the number 3. I_0 nearly doubles with every 10 °C rises in temperature for silicon PV panels near room temperature. By substituting the equation for I_0 into the equation for V_{OC}, as shown below, the effect of I_0 on the open-circuit voltage can be calculated:

$$V_{OC} = \frac{kT}{q}ln\left(\frac{I_{SC}}{I_O}\right) = \frac{kT}{q}[\ln I_{SC} - \ln I_O]$$
$$= \frac{kT}{q}\ln I_{SC} - \frac{kT}{q}ln\left[B'T^\gamma exp\left(-\frac{qV_{GO}}{kT}\right)\right] =$$
$$\frac{kT}{q}\left(\ln I_{SC} - \ln B' - \gamma \ln T + \frac{qV_{GO}}{kT}\right) \quad (5)$$

where $E_{GO} = qV_{GO}$. Assuming that dVoc/dT does not depend on dIsc/dT, dVoc/dT can be found as:

$$\frac{dV_{OC}}{dT} = \frac{V_{OC} - V_{GO}}{T} - \gamma\frac{k}{q} \quad (6)$$

The above equation demonstrates that a PV panel's temperature sensitivity is proportional to its open-circuit voltage V_{oc}, with higher voltage PV panels being less affected by temperature. E_{Go} is 1.2 for silicon, and setting γ to be 3 reduces the open-circuit voltage V_{oc} by around 2.2 mV/°C:

$$\frac{dV_{OC}}{dT} = -\frac{V_{GO} - V_{OC} + \gamma\frac{kT}{q}}{T} \approx -2.2mV \ per \ °C \ for \ Si \quad (7)$$

Since the bandgap energy, E_G, decreases with temperature, more photons have enough energy to build e-h pairs, the short-circuit current, I_{SC}, increases slightly. However, this is a minor consequence, as shown in equation (8), which shows the temperature dependence of the short-circuit current from a silicon photovoltaic cell:

$$\frac{1}{I_{SC}}\frac{dI_{SC}}{dT} \approx 0\cdot 0006 \ per \ °C \ for \ Si \quad (8)$$

or ≈0.06% per °C for silicon.

The following equation approximates the temperature dependence FF for silicon:

$$\frac{1}{FF}\frac{dFF}{dT} \approx \left(\frac{1}{V_{OC}}\frac{dV_{OC}}{dT} - \frac{1}{T}\right) \approx -0\cdot 0015 \ per \ °C \ for \ Si \quad (9)$$

The following is the impact of changing temperature dT on maximum power output, P_M:

$$P_{Mvar} = \frac{1}{P_M}\frac{dP_M}{dT} = \frac{1}{V_{OC}}\frac{dV_{OC}}{dT} + \frac{1}{FF}\frac{dFF}{dT} + \frac{1}{I_{SC}}\frac{dI_{SC}}{dT} \quad (10)$$

$$\frac{1}{P_M}\frac{dP_M}{dT} \approx -(0 \cdot 004 \ to \ 0 \cdot 005) \ per \ °C \ for \ Si \qquad \text{or } 0.4\% \text{ to}$$

0.5% per °C for silicon. (11)

C. Effect of solar Irradiance

The predicted rise in reflected irradiance would result in an increase in generated power by increasing the PV module's short circuit current (Isc). As a response to the PV module, while a higher light intensity has fallen on its surface, A positive effect on the short circuit current of the module will take place. All photovoltaic cell parameters, including the, short-circuit current, and the open-circuit voltage are affected by the amount of light incident on the cell. [23]

1) *The effect of concentration on a PV cell's IV characteristics*

The series resistance has a greater impact on cell output when the light intensity is high, while the shunt resistance has a greater impact when the light intensity is low. A solar cell short-circuit current is proportional to the light intensity, so a device operating under ten suns would have ten times the short-circuit current of a device operating under one sun. However, since incident power increases linearly with concentration, this effect does not increase the efficiency of the PV panel. Instead, the logarithmic dependence of the open-circuit voltage on the short circuit is responsible for the efficiency gains. V_{oc} increases logarithmically with light intensity under concentration, as in the equation below:

$$V'_{OC} = \frac{nkT}{q}ln\left(\frac{X \ I_{SC}}{I_O}\right) = \frac{nkT}{q}\left[ln\left(\frac{I_{SC}}{I_O}\right) + lnX\right] = V_{oc} + \frac{nkT}{q}\ln X$$

(12)

Where X is the concentration of sunlight.
From equation (12), a doubling of the light intensity (X=2) causes an 18 mV rise in V_{OC}.

The Sandia PV Array Performance Model (SAPM) defines five points on the IV curve. These points are shown in the figure below. Fig.4.
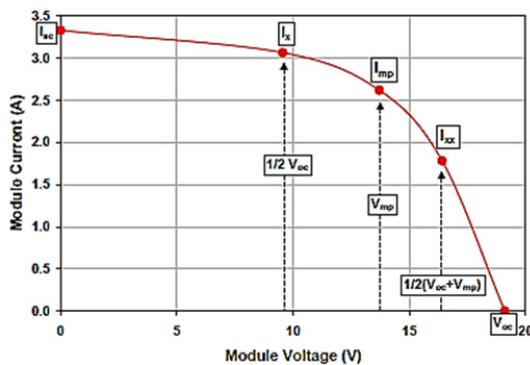

Fig.4. The SAPM defines the primary points (Isc, Imp, Voc, Vmp) with the following equations

$$I_{SC} = I_{SC0} * \mathcal{F}_1\left(\frac{E_b\mathcal{F}_2+\mathcal{F}_dE_d}{E_0}\right) * \left(1 + \alpha_{Isc}(T_C - T_0)\right) \quad (13)$$

$$I_{mp} = I_{mp0}(C_0E_e + C_1E_e^2)\left(1 + \alpha_{Imp}(T_C - T_0)\right) \quad (14)$$

$$V_{OC} = V_{OC0} + N_s\delta ln(E_e) + \beta V_{OC}(T_C - T_0) \quad (15)$$

$$V_{mp} = V_{mp0} + C_2N_s\delta ln(E_e) + C_3N_s(\delta ln(E_e))^2 +$$

$$\beta V_{mp}(T_C - T_0) \qquad (16)$$

where

- $\mathcal{F}_1$ is a 4th order polynomial function of the absolute <u>air mass</u>, AM_a, and is called the air mass modifier.
- $\mathcal{F}_2$ is a 5th order polynomial function of angle of incidence, AOI, and is called the <u>angle of incidence modifier</u>.
- E_b is beam irradiance on the plane of the array
- E_d is the diffuse irradiance on the plane of the array
- E_0 is reference solar irradiance (1000W/m²)
- T_C is cell temperature (°C)
- T_0 is reference cell temperature (25 °C)
- $\mathcal{F}_d$ is the fraction of the diffuse light that is used by the module. For typical flat plate modules $\mathcal{F}_d$ is usually assumed to be equal to 1. For concentrators, the value can be smaller than 1.
- α_{Isc} is the normalized temperature coefficient for short circuit current. Units are 1/°C
- α_{Imp} is the normalized temperature coefficient for maximum power current. Units are 1/°C
- N_s is the number of cells in series
- C is a vector of coefficients determined by module testing using a method developed at Sandia.

- E_e is the "effective irradiance". It is defined as:

$$E_e = \frac{I_{sc}}{I_{sc0}\{1+\alpha I_{sc}(T_C-T_0)\}} \qquad (17)$$

where:
- I_{sc0} is the short circuit current at reference conditions.
- I_{SC} can be calculated from (eq. 1) above.
- δ is a function of T_C defined as:

$$\delta = \frac{n*k(T_C+273\cdot15)}{q} \qquad (18)$$

where:
- n is an empirically determined 'diode factor',
- k is Boltzmann's constant (1.38066 x 10⁻²³ J/K),
- q is the elementary charge constant (1.60218 x 10⁻¹⁹ Coulomb)
- βV_{OC} is a function of <u>effective irradiance</u>, E_e, defined as:

$$\beta V_{OC} = \beta V_{OC0} + m\beta V_{OC}(1 - E_e) \qquad (19)$$

where:

- βV_{OC0} is the temperature coefficient for module open-circuit voltage at irradiance conditions of 1000W/m²

- $m\beta V_{OC}$ is a coefficient describing the irradiance dependence for the open-circuit voltage temperature coefficient (typically equals zero).

A proportional dimension of planar concentrator will be installed at the open solar outdoors test field on the top roof of the Faculty of Engineering, Heliopolis University for Sustainable Development (30°09'11.7"N 31°25'57.4"E). 3 groups of PV modules were arranged in front of the wide planar reflectors, and their actual locations concerning the reflector are shown in (Fig.5&6). The tilt angles of the reflecting surfaces from horizontal were initially ø =10◦ and PV modules angles ω =30◦.

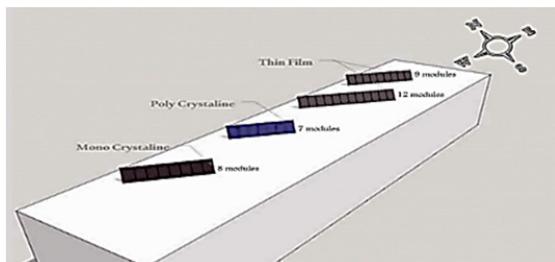Fig.5 Proposed fixing of the reflectors

Fig.6 Orientation of the PV panels on the top roof of the building

III. EXPERIMENTAL RESULTS AND DISCUSSION

A set of control modules with no reflectors were installed at the same module tilt angle and at a tilt angle of 30 to match the optimal tilt angle for the region.

Meteorological measurements were made by the Meteo Station (Fig.7) Appendix-A which is a device for measuring power-related meteorological data at the PV plant location and for transmitting this data to the Sunny WebBox via the Power Injector.

The Meteo Station fulfills the following tasks:

• Measurement of global radiation
• Measurement of PV cell temperature
• Measurement of absolute air pressure
• Measurement of air temperature and humidity
• Transmission of this meteorological data to the Sunny WebBox.

All measurements were taken at the site. The modules were monitored for short-circuit current (I) and the temperature at the top and bottom of the module. The concentration system

will be installed using 1 type of reflector: 1- commercial reflector (semi-diffuse, flexible reflector made of an aluminized PET laminate, (Foylon). Consists of 3 layers, Polyester with a thickness (12 micrometers) + Aluminium with the thickness (7 micrometers) + Polyethylene with the thickness (80 micrometers) Commercially it's written: Pet/alu/pe 12/7/80 mic.

Fig.7 SMA Meteo Station

Which is preferred because of the protective layer of Polyethylene. It should be noted that both modules and reflectors should be cleaned of any major soiling and organic depositions when they were observed.

The incident illumination on reflectors is based on the sun's azimuth and elevation angle. This process could be repeated for the entire year to calculate the cumulative amount of annual yield power. We can estimate the amount of power for a specific model design. Further calculations can be performed for different system designs (e.g., reflector tilting for other angles by simply repeating the above process). In addition to absolute power density, to obtain an optimum model configuration, the irradiance distribution on PV modules must be studied. Since the fixed PV panels were augmented by reflectors throughout the day, the occurrence of a uniform irradiance distribution on modules is expected. The uniformity issue is an important factor to fully study power production capability and estimate degradation rates. The output generated power curves were collected from the system log files then we could use it to compare the results after using reflectors.

A. Logged data to be used

A logged data was registered to be used in comparison for both systems before and after using the reflectors.

The weather data (solar Irradiance, ambient and module temperature), and PV system instantaneous power were acquired from the weather meters (Pyrometers & Thermometer) and solar panels located at Heliopolis University for sustainable development campus, Faculty of Engineering building. The global solar irradiance, ambient

temperature, module temperature, I_{PV}, V_{PV}, and specified data of output power were recorded and stored starting from the year 2013 till now, the last 2 years' data 2018, and 2019 was taken as a reference from 1st of January 2018 to 31st of December 2019 with the sampling one hour.

The PV model and solar model were used for the determination of the power generation from the photovoltaic panel for location coordinates: 30°09'11.7"N 31°25'57.4"E., Cairo, Egypt. In Fig.1 The local monthly average ambient temperature T base on the measurement, and, the monthly average daily solar radiation together with clearness index are presented. The PV power output directly depends on the amount of radiation incident on the surface of the PV array and array temperature.

The following are samples of the used data as the real records to be an input for the simulated model to predict the output power after using the reflectors for the 3 types of PV module.

1) Total yield energy (kWh) for the year 2019 for the 3 types of modules without reflectors.

2) Total yield Energy for the year 2018 for the 3 types of modules without reflectors.

3) Average of the total yield energy for the 3 types of modules for the years 2018,2019.

4) A typical result of one day for the generated power (kW) of each of the 3 types of PV modules. Fig.8

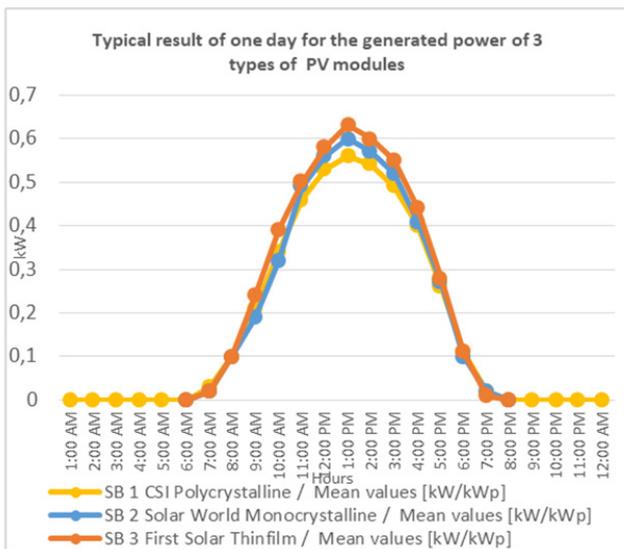

Fig.8 typical result of one day for the generated power (kW) of each of the 3 types of PV modules

5) Average of the total yield energy for the thin-film modules for the years 2018, 2019.

6) Average of the total yield energy for the monocrystalline modules for the years 2018, 2019 Fig.9.

7) Average of the total yield energy for the Polycrystalline modules for the years 2018, 2019

8) A total Irradiance & ambient Temperatures results for the year 2019. Fig.10.

9) Total Irradiance & ambient Temperatures results for the year 2018.
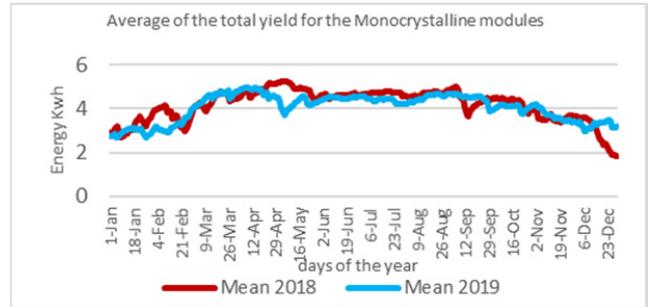

Fig.9 Average of the total yield for the Monocrystalline modules for the years 2018, 2019
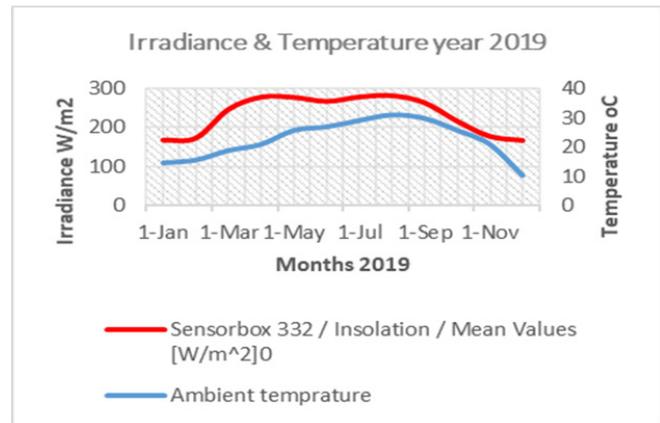

Fig.10 A total Irradiance & ambient Temperatures results for the year 2019

IV. MODELING PROCESS

A MATLAB Simulink PV model was implemented with the same specs as the real PV system which was built on the top roof of the building of the Faculty of Engineering, Heliopolis University. with the same orientation and the input parameters was taken from the recorded data which already registered of that system.

All input parameters are the real parameters to simulate real conditions applied to the implemented PV system to make the comparison between the simulated output data after applying the reflectors and the real output data before applying the reflectors are closest to the real situation.

A model of a numerical simulation of a stationary solar field augmented by plane reflectors: optimum design parameters to predict the amount of reflected irradiance from the reflector was used based on the dimension of the reflector rational with the dimension of the PV module. Fig. 11. [23]
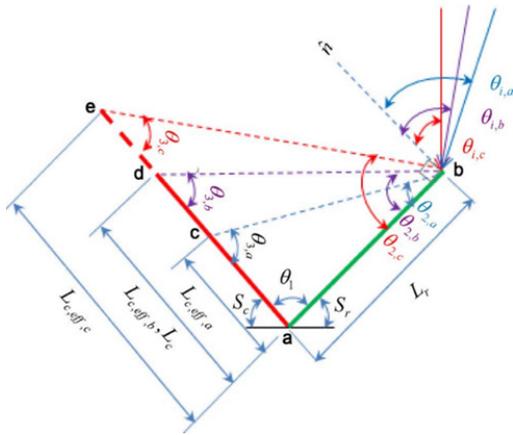
Fig.11 Incidence beam of solar radiation onto the reflector and the PV panel (red arrows) and reflected from the reflector onto the PV panel (blue arrows)

A. Solar Irradiance components calculation

To calculate the diffused irradiance from the reflector: for all irradiances $(I^t_{c, T})$ that strike the PV module's surface, expressed as:

$$I^t_{c.T} = (I^t_b + A^t_i I^t_d)\left[R^t_{b.c} + \frac{L_r}{L_c}\frac{L^t_{c.eff}}{L_c}Q_r R^t_{b.r\to c}\right] + (1 - A^t_i)I^t_d\left[F_{c-sky} + \frac{L_r}{L_c}Q_r F_{r-sky}F_{c-r}\right] \quad (20)$$

where:

$R^t_{b.c}$. $R^t_{b.r\to c}$ are the geometric factors, Q_r is the reflectivity of the reflector,= Reflectivity can be calculated as $Q_r = Gr(y)/Gi(y)$ where Q is the reflectivity= 0.85 for the used reflector., y is the wavelength of the light, G_r is the reflected radiation and G_i is the incident radiation. ≈0.36 percent

$$R^t_{b.c} = \frac{cos\theta^t_{i.c}}{cos\theta^t_z} \quad , \quad R^t_{b.r\to c} = \frac{cos\theta^t_{i.r\to c}}{cos\theta^t_z} \quad (21)$$

Diffuse reflection is the most common type of reflectivity and occurs when light strikes rough surfaces, such as pavement, foliage, clothing, and vehicles. These surfaces cause the light beams to scatter in all directions. An only a small amount of the light is reflected toward the source. Fig.12
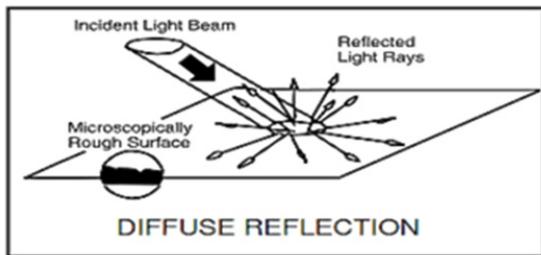

Fig.12. Diffuse Reflection

The values of the reflector height to the PV module height ratio $(\frac{L_r}{L_c})$ and the reflected tilted angle (S_r) are calculating according to the field design parameters: $(S_c, \frac{X}{L_c})$ the collector tilted angle, and the distance separating the rows to the

collector height ratio, respectively. the reflector tilt angle is given by:

$$S_r = tan^{-1}\left[\frac{sin\,S_c}{\frac{X}{L} - cos\,S_c}\right] \quad (22)$$

And the reflector to PV module height ratio is calculated from the following:

$$\frac{L_r}{L_c} = \frac{sin\,S_c}{sin\,S_r} \quad (23)$$

The variation of the reflector parameters $(S_r, \frac{L_r}{L_c})$ concerning the solar field parameters $(S_c, \frac{X}{L_c})$ is calculated

F_{c-sky} : collector (PV module)-sky view factor:

$$F_{c-sky} = 0\cdot 5\left[1 + \frac{X}{L_c} - \sqrt{1 + \left(\frac{X}{L_c}\right)^2 - 2\frac{X}{L_c}cos\,S_s}\right] \quad (24)$$

F_{r-sky} : reflector-sky view factor:

$$F_{r-sky} = \frac{\left[\frac{L_r}{L_c} + \frac{X}{L_c} - \sqrt{\left(\frac{L_r}{L_c}\right)^2 + \left(\frac{X}{L_c}\right)^2 - 2\frac{X}{L_c}\frac{L_r}{L_c}cos\,S_r}\right]}{2\frac{L_r}{L_c}} \quad (25)$$

F_{c-r} : collector-reflector view factor by using the view factor algebra can be presented by:

$$F_{c-r} = 1 - F_{c-sky} \quad (26)$$

By using the above calculations to calculate the new value of the diffused irradiance after using the reflectors, then applying the result as a diffused extra irradiance as an input with the other recorded environmental data to the simulated PV system using the prepared model, putting under consideration the temperature co-efficient of the PV module which can be assigned as a factor for V_{pv} & I_{PV} for the used panels for each type of the 3 types of the used PV modules. thus, a very important factor, because after installing the reflectors to the PV system an increase in temperature of the module was expected. then the effect of that expected heat will be calculated and be taken under a consideration.

V. SIMULATED RESULTS

As a result of a simulation model, the following are just sample of the whole data which could be obtained from the simulation model. Two main groups of the results were obtained, a) A control PV panels without adding the reflectors used as a control (reference) panel. b) PV panels after adding the reflectors to be used as a result of this research point.

- A simulation of a normal day in January before using the reflectors as an input (Irradiance and Ambient temperature) and output (the PV modules current Ipv, the PV modules voltage Vpv, and the generated output power Ppv) for the Thin Film modules type. Fig.13.
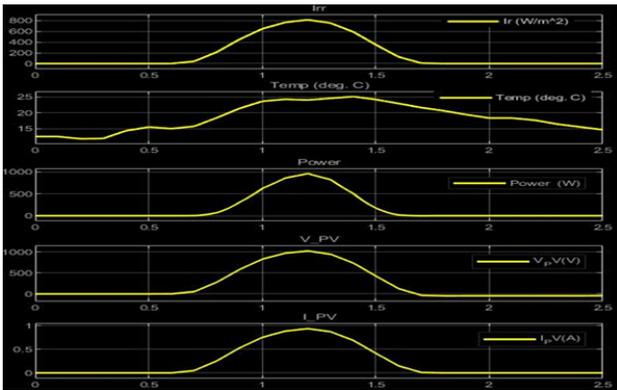
Fig. 13 Control Thin Film modules output (January)

- A simulation of a normal day in August before using the reflectors as an input (Irradiance and Ambient temperature) and output (the PV modules current I_{pv}, the PV modules voltage V_{pv}, and the generated output power P_{pv}) for the Thin Film modules type. Fig.14
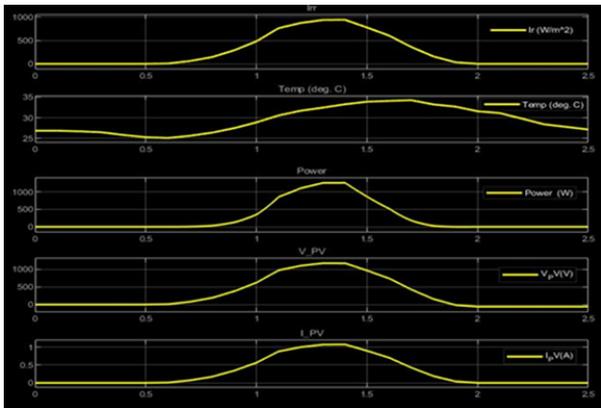

Fig. 14 Control Thin Film modules output (August)

A simulation of a normal day in January after using the reflectors as an input (Irradiance and Ambient temperature) and output (the PV modules current Ipv, the PV modules voltage Vpv, and the generated output power Ppv) for the Thin Film modules type. Fig.15.
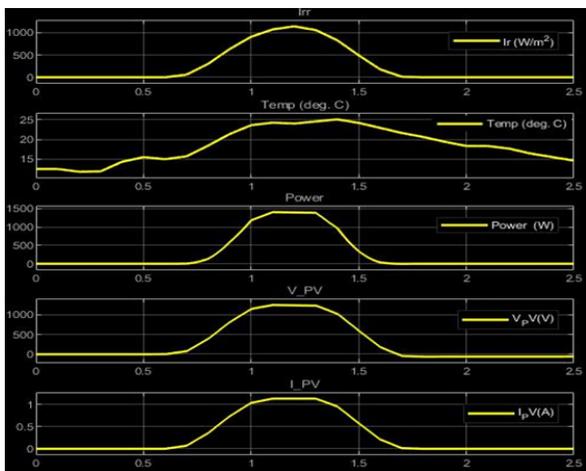

Fig. 15 Thin Film modules output with reflector (January)

From Fig.27 it could be noticed that the top area of the output power curve seems to be a flat edge, it's because the PV modules have a limit maximum output which is 1470w in the case of Thin-film modules, then although the higher in input irradiance but the maximum power can't exceed than the maximum limit of the panels, on the other hand, the total area under the power curve was increased.

- A simulation of a normal day in August after using the reflectors as an input (Irradiance and Ambient temperature) and, output (the PV modules current Ipv, the PV modules voltage Vpv, and the generated output power Ppv) for a Thin Film modules type. Fig.16.
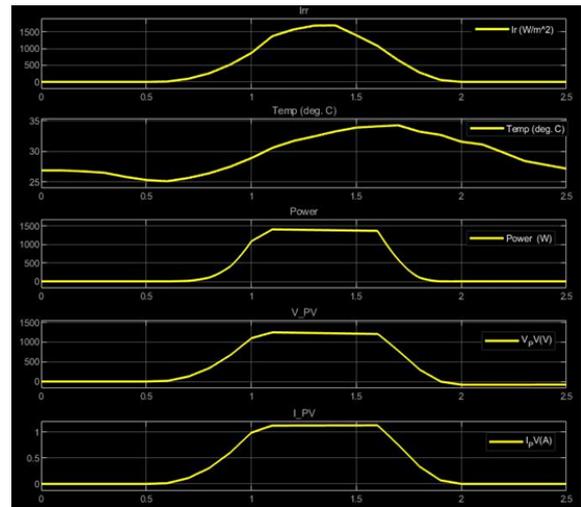

Fig. 16 Thin Film modules output with reflector (August)

from the above graph, it could be noticed that the top area of the output power curve seems to be a flat edge, it's because the PV modules have a limit maximum output which is 1470w in the case of Thin-film modules, then although the higher in input irradiance but the maximum power can't exceed than the maximum limit of the panels, on the other hand, the total area under the power curve was increased, also it is very clear that the flat area on top of the power curve was much more linger than the same curve in January that's mean the losses of an extra generated power is much higher in summer times.

- From the above results we can simplify the changes in the output power before and after using the reflectors for the 3 types of PV modules as the following:

a) Comparison between the output power before using the reflectors (blue), and after using the reflectors (red). in the **Thin-film** modules in **January**, a flat area on top of the red graph after using the reflectors is very clear, which means that the output power of the modules is reached the maximum output of the PV modules at the noontime which is Total Power for the panels: 1470 W. also a slightly increasing in power could be happened in the early morning and at the late time before sunset. Fig.17.
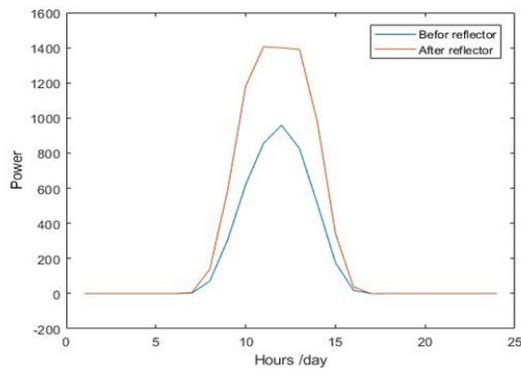
Fig. 17 Thin film power output in January before (blue), and after (red), using reflectors Power ratio = 1.7169

b) Comparison between the output power before using the reflectors (blue), and after using the reflectors (red). in the **Thin-film** modules in **August**, a flat area on top of the red graph after using the reflectors is very clear, which means that the output power of the modules is reached the maximum output of the PV modules at noontime which is Total Power for the panels: **1470 W.** also a recognized increase in power could be happened in the early morning and at the late time before sunset. Fig.18
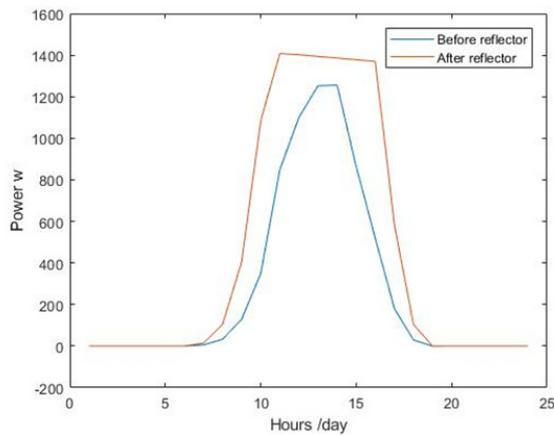

Fig. 18 Thin film power output in August before (blue), and after (red), using reflectors Power ratio = 1.6193

c) Comparison between the output power before using the reflectors (blue), and after using the reflectors (red). in the **Monocrystalline** modules in **January**, a flat area on top of the red graph after using the reflectors is very clear, which means that the output power of the modules is reached to the maximum output of the PV module at the noontime Total Power for the panels: **1400W**. also, a slight increase in power could happen in the early morning and at the late time before sunset. Fig.19

d) Comparison between the output power before using the reflectors (blue), and after using the reflectors (red). in the **Polycrystalline** modules in **January**, a flat area on top of the red graph after using the reflectors is very clear, which means that the output power of the modules is reached the maximum output of the PV module at the noontime Total Power for the panels: **1645 W**. also a slightly increasing in

power could be happened in the early morning and at the late time before sunset. Fig.20
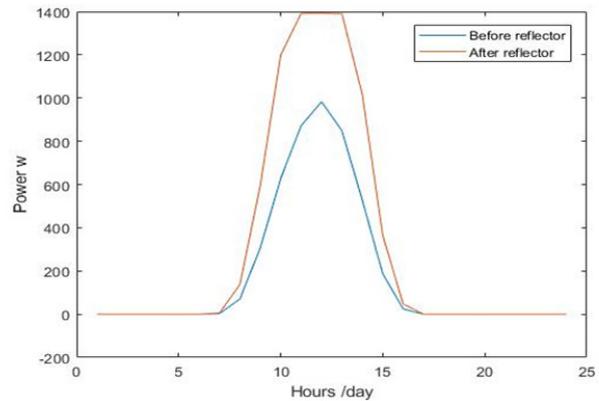

Fig. 19 Monocrystalline power output in January before (blue), and after (red), using reflectors Power ratio = 1.6943
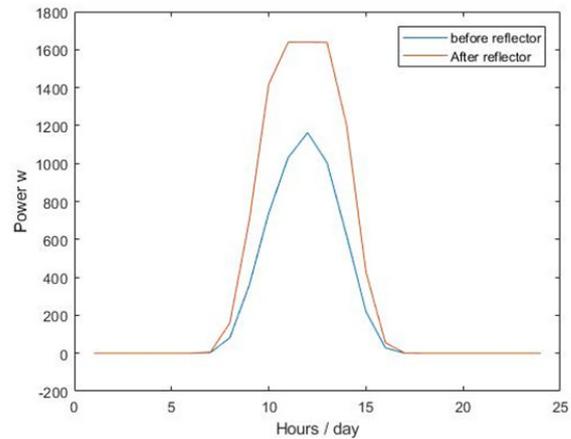

Fig. 20 Polycrystalline power output in January before (blue), and after (red), using reflectors Power ratio = 1.6931

A full data for the output power has been registered for the 3 types of PV panels (Monocrystalline, Polycrystalline, and Thin-film) for all cases before and after adding the reflectors to the modules.

Samples of the registered data for the power before adding the reflector was registered for all the 3 types of the PV panels can be presented as the following in Table II.

TABLE II OUTPUT POWER BEFORE ADDING REFLECTORS FOR THE THREE TYPES OF PV MODULES

Month	Monocrystalline	Polycrystalline	Thin film
January	4.449	5.251	4.348
April	7.714	9.1119	7.6989
August	6.664	7.895	6.568

Samples of the registered data for the power after adding the reflector was registered for all the 3 types of the PV panels can be presented as the following in Table III.

TABLE III. OUTPUT POWER AFTER ADDING REFLECTORS FOR THE 3 TYPES OF PV MODULES

Month	Monocrystalline Power ratio	Polycrystalline Power ratio	Thin film Power ratio
January	7.539	8.890	7.466
April	9.871	11.646	9.91926276
August	10.483	12.364	10.635

A total yield power for a complete one year for Thin-film modules before and after adding the reflectors can be presented in the following chart. Fig 21.
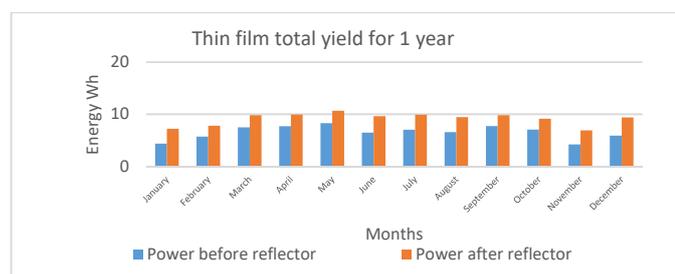

Fig. 21 Thin film total yield for 1 year

Samples of the registered data for the power ratio for all the 3 types of PV panels can be presented as the following Table IV.

TABLE IV. POWER RATIO SAMPLES FOR THE 3 TYPES OF PV PANELS

Month	Monocrystalline Power ratio	Polycrystalline Power ratio	Thin film Power ratio
January	1.6943	1.693	1.716
April	1.2796	1.2781	1.2884
August	1.5729	1.566	1.6193

A graph of the registered data for the power ratio for Thin-film type for one year of the PV panels can be presented as the following. Fig. 22.
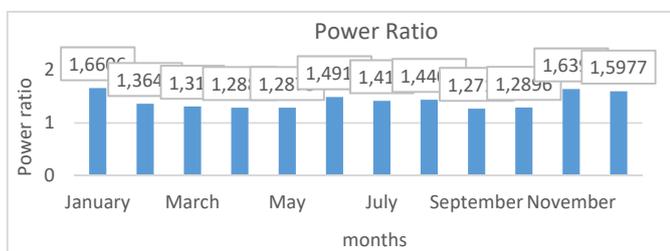

Fig. 22 Power ratio samples for the 3 types of PV panels

From the above-collected data, a generated power yield for Thin-film modules through a year before and after applying reflectors could be presented in the following table. Table V.

TABLE V. COLLECTED DATA FOR THE POWER YIELD FOR THIN-FILM MODULES FOR A TOTAL OF ONE YEAR

	Energy before reflector Wh	Energy after reflector Wh	Power Ratio
January	4.348	7.2202888	1.6606
February	5.703	7.7800326	1.3642
March	7.4792	9.8052312	1.311
April	7.6989	9.91926276	1.2884
May	8.2869	10.66772637	1.2873
June	6.4566	9.62872758	1.4913
July	6.9983	9.9095928	1.416
August	6.568	9.4598904	1.4403
September	7.7238	9.81926694	1.2713
October	7.0689	9.11605344	1.2896
November	4.1916	6.87254736	1.6396
December	5.88	9.394476	1.5977

VI. CONCLUSION

One of the most effective ways to drive down the cost of PV electricity is to install reflectors with PV panels to harvest more light from the modules. by increasing the output rate with the approximate value from about 35% - 45%

Theoretically, this paper approved that both monocrystalline and polycrystalline PV modules slightly have a difference in the output power ratio, monocrystalline PV module is slightly higher in the output power, but for the whole types, the Thin-film PV module is the most higher in the value of its generated power, the highest average power ratio for the whole 3 types for the Thin-film modules is equal to (1.421441667) which means that the output power after installing the reflectors is increased by about 42% from the basic output.

This method is one of the cheapest and easiest ways to increase the power of PV panels, adding to that, the reflecting plates system is lower in cost than adding more solar PV panels. The effect of increasing the temperature could be detected very clearly in the slight decay of the open-circuit voltage value (V_{oc}), which could be neglected if it compared with the increasing of the short circuit current (I_{SC}), that's mean the increasing of the output power is compensating that shortage of the open-circuit voltage as a result of increasing the temperature of the module.

VII. FUTURE WORK

Implementing a reflector panels system adding it to the current PV system to try to compare the practical results with the theoretical results. running stage Fug..22-23-24-25

Study the results of adding another 2 types of reflectors to study the behavior of the generated output power for the 3 types of PV modules. the reflectors could be like the following 1- White paint high gloss. 2- Tyvek material.

Separately study the effect of the temperature on each type of the 3 types of PV modules (Monocrystalline,

Polycrystalline, and Thin Films) which is a very important parameter for those who are implementing a PV solar system in the hot environmental weather.
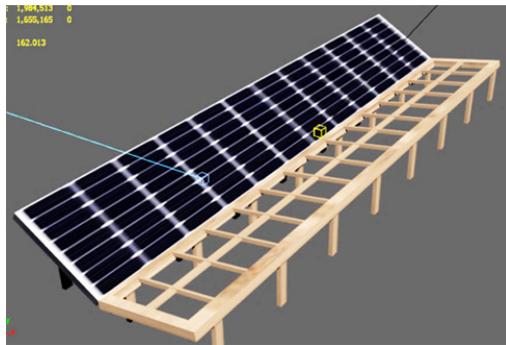

Fig.22 3D design of the reflectors

Fig.23 Implementing stage of the reflectors

Fig.24 Fixing stage of the reflectors

Fig.25 Final stage of the reflectors

REFERENCES

[1] Performance Comparison of Mirror Reflected Solar Panel with Tracking and Cooling Sheikh Md. Shahin Alam1, Dr. A.N.M. Mizanur Rahman*21UG Student,2ProfessorDepartment of Mechanical Engineering Khulna University of Engineering & Technology, Khulna-9203, Bangladesh (14) (PDF) Performance comparison of mirror reflected solar panel with tracking and cooling. Conference: 2016 4th International Conference on the Development in the in Renewable Energy Technology (ICDRET)

[2] Budiyanto, Fadliondi Department of Electrical Engineering, University as Muhammadiyah Jakarta, Indonesia International Journal of Power Electronics and Drive System (IJPEDS) September 2017

[3] Photovoltaic System Performance Enhancement with Non-Tracking Planar Concentrators: Experimental Results and Bi-Directional Reflectance Function (BDRF) Based Modelling Rob W. Andrews, Andrew Pollard, and Joshua M. Pearce IEEE JOURNAL OF PHOTOVOLTAICS, VOL. 5, NO. 6, NOVEMBER 2015.

[4] Photovoltaic System Performance Enhancement with Non-Tracking Planar Concentrators: Experimental Results and BDRF Based Modelling. Rob W. Andrews ,Andrew Pollard and Joshua M. Pearce Department of Mechanical and Materials Engineering Queen's University, Kingston, Ontario, Canada Department of Materials Science and Engineering and the Department of Electrical and Computer Engineering Michigan Technological University, Houghton, MI, USA 2013.

[5] Solar-concentrating photovoltaic mirror, Arizona state university (USA) PV mirror: a solar concentrator mirror incorporating PV cells 2017

[6] An experiment of improvement in solar panel efficiency using solar concentration by the number of mirrors. Ranjan Alok et. al; International Journal of Advance Research, Ideas, and Innovations in Technology 2018.

[7] Efficiency Improvement of a Typical Solar Panel with the Use of Reflectors. GDM Pathmika and MV Gamage Department of Mechanical Engineering, Faculty of Engineering, Sri Lanka Institute of Information Technology (SLIIT), 2016.

[8] Enhancement Efficiency of Solar Cell using Simple Mirror Technique. Pooja R. Tandale ,Dr. Sanjay Mohite, P.G. Student, Department of Electronics and Telecommunication, JSPM's JSCOE, Pune, India Associate Professor, Department of Electronics and Telecommunication, JSPM's JSCOE, Pune, India. 2017.

[9] Increasing the Output Power and Efficiency of Solar Panel by Using Concentrator Photovoltaics (CPV). Muhammad Bilal, Muhammad Naeem Arbab, Muhammad Zain Ul Abideen Afridi, Alishpa Khattak. 2017

[10] Performance Evaluation of Photovoltaic Solar System with Different Cooling Methods and a Bi-Reflector PV System (BRPVS): An Experimental Study and Comparative Analysis. Muhammad Adil Khan and Hee-Je Kim ,Byeonghun Ko ,Esebi Alois Nyari ,and S. Eugene Park. 2017.

[11] The experiment of double solar energy by reflection light method. S. Julajaturasirarath, W. Jonburom, N. Pornsuwancharoen. a Nano Photonics Research Group, Department of Electrical Engineering, Faculty of Industry and Technology, Rajamangala University of Technology Isan, Sakon Nakhon Campus, Sakon Nakhon, 47160, Thailand advance Research Center for Photonics. Faculty of Science, King Mongkut's Institute of Technology Ladkrabang, Bangkok, 10520 ,Thailand Elsevier use only: Received 30 September 2011; Revised 10 November 2011; Accepted 25 November 2011.

[12] Mirror-Augmented Photovoltaic Designs and Performance. Wei-Chun Lin, Dave Hollingshead, Kara A. Shell, Joseph Karas, Scott A. Brown, Mark Schuetz, Yang Hu, and Roger H. French, Member, IEEE. 2012.

[13] Design and implementation of the solar tracker with reflected mirrors. A.SUNIL & V.PRAVEEN KUMAR Department of Mechanical Engineering, SBIT, Haryana, India. 2016.

[14] The Solar ATLAS of Egypt. The geo-cradle project received funding from the European union's horizon 2020 research and innovation program under grant agreement no 690133. 2018.

[15] Photovoltaic Efficiency: Concentrated Solar Power Fundamentals Article. 2018.

[16] Effect of Angle Orientation of Flat Mirror Concentrator on Solar Panel System Output. Assist. Prof Dr. Ali H.AL-Hamadany, Assist.

Prof. Dr. Faten Sh. Zain Al-Abideen, Jinnan H. Ali, University of Technology/Renewable Energy Research Center, Almustansiriyah University /Education College/Physics Department, Baghdad Governorate. 2016.

[17] A cost-effective theoretical novel configuration of a concentrated photovoltaic system with linear fresnel reflectors. Calik K., Firat C., "A cost-effective theoretical novel configuration of a concentrated photovoltaic system with linear fresnel reflectors ", Politeknik Dergisi, 22(3): 583-589, (2019).

[18] Investigation of soiling effect on different solar mirror materials under Moroccan climate. A.Alami Merrounia , F.Wolfertstetterb , A.Mezrhaba , S.Wilbertb , R.Pitz-Paal. International Conference on Concentrating Solar Power and Chemical Energy Systems, Solar PACES 2014.

[19] Solar Cells: In Research and Applications—A Review. Shruti Sharma1, Kamlesh Kumar Jain, Ashutosh Sharma, CMD College, Bilaspur, India, Materials Science and Engineering, University of Seoul, Seoul, South Korea. published 24 December 2015.

[20] Lightweight Carbon Fiber Mirrors for Solar Concentrator Applications. Nina Vaidya1, Michael D. Kelzenberg1, Pilar Espinet-Gonzalez1, Tatiana G. Vinogradova1, 2, Jing-Shun Huang1, Christophe Leclerc1, Ali Naqavi1, Emily C. Warmann1, Sergio Pellegrino1, Harry A. Atwater1 1 California Institute of Technology, Pasadena, CA 91125, United States 2 Northrop Grumman Aerospace Systems, Azusa, CA 91702, United States. 2016.

[21] A Simple Approach in Estimating the Effectiveness of Adapting Mirror Concentrator and Tracking Mechanism for PV Arrays in the Tropics. M. E. Ya'acob, Myo Than Htay H. Hizam, H. Abdul Rahman, andA.H.M.A.Rahim. Z. Wan Omar.2014

[22] M. Nakamura, Yamaguchi, K., Kimoto, Y., Yasaki, Y., Kato, T., and Sugimoto, H., "Cd-Free Cu(In, Ga)(Se, S)2 Thin-Film Solar Cell With Record Efficiency of 23.35%", IEEE Journal of Photovoltaics, vol. 9, pp. 1863-1867, 2019.

[23] A Numerical Simulation of a Stationary Solar Field Augmented by Plane Reflector: Optimum Design Parameters. Samer Yassin Alsadi , Yasser Fathi Nassar, Electrical Engineering Department, Faculty of Engineering and Technology, Palestine Technical University-Kadoorie, Tulkarm, Palestine Mechanical Engineering Department, Faculty of Engineering and Technology, Sebha University, Brack El-Shati, Libya. July 6, 2017.

[24] The mathematical model for the power generation from the arbitrarily oriented photovoltaic panel. Qusay Hassan, Marek Jaszczur Estera, Przenzak, Department of Fundamental Research in Energy Engineering, Faculty of Energy and Fuels, AGH University of Science and Technology, Poland, Department of Sustainable Energy Development, Faculty of Energy and Fuels, AGH University of Science and Technology, Poland 2017.

[25] F. Hong, Lin, W., Meng, W., and Yan, Y., "Trigonal Cu 2 -II-Sn-VI 4 (II = Ba, Sr, and VI = S, Se) quaternary compounds for earth-abundant photovoltaics", Phys. Chem. Chem. Phys., vol. 18, no. 6, pp. 4828 - 4834, 2016.DOI Google Scholar BibTeX RTF Tagged MARC EndNote XML RIS. 2016.

[26] T. Feurer et al., "Progress in thin-film CIGS photovoltaics–Research and development, manufacturing, and applications", Progress in Photovoltaics: Research and Applications, vol. 25, pp. 645–667, Google Scholar BibTeX RTF Tagged MARC EndNote XML RIS. 2017.

[27] M. Nakamura, Yamaguchi, K., Kimoto, Y., Yasaki, Y., Kato, T., and Sugimoto, H., "Cd-Free Cu(In,Ga)(Se,S)2 Thin-Film Solar Cell With Record Efficiency of 23.35%", IEEE Journal of Photovoltaics, vol. 9, pp. 1863-1867, 2019.DOI Google Scholar BibTeX RTF Tagged MARC EndNote XML RIS. 2019.